A substituted BF_2-chelated tetraarylazadipyrromethene as an intrinsic dual chemosensor in the 650–850 nm spectral range

John Killoran,[a] Shane O. McDonnell,[a] John F. Gallagher[b] and Donal F. O'Shea*[a]

Received (in Durham, UK) 24th August 2007, Accepted 13th November 2007
First published as an Advance Article on the web 20th November 2007
DOI: 10.1039/b713020a

The synthesis and spectral analysis of a new class of long wavelength intrinsic fluorosensor is reported. Chemosensor performance reveals large off/on fluorescence intensity responses to acid analyte with low response to microenvironment polarity. Application to ratiometric fluorescence/UV-visible analysis is outlined.

Introduction

The development of organic chromophores with spectral properties in the near-infrared (NIR) and visible red spectral regions continues to attract a sustained research interest. New chromophore scaffolds with controllable photophysical properties in the 650–900 nm spectral region offer potential for exploitation in a diverse range of material and biological applications, such as optical data storage,[1] photoconductors,[2] electrochromic devices,[3] chemosensors,[4] immunoassay labels and bioconjugated probes,[5] and *in vitro* and *in vivo* imaging agents.[6] Specifically, NIR dyes are suitable as *in vitro* and *in vivo* biomedical diagnostic agents due to efficient penetration of light through tissue and the low auto-fluorescence of endogenous chromophores in this spectral region.[7] Despite the optical benefits of utilising this spectral region for analytical techniques, there is a surprising scarcity of organic compounds which have the desired absorption and emission properties. In spite of their poor photostability and lengthy synthetic routes, the cyanine dyes have to date been the most widely utilised class for applications in this spectral region.[8]

We are currently interested in devising new chemosensors based upon the BF_2-chelated-azadipyrromethenes, which are readily synthesised, show high photostability, and are amenable to peripheral functionalisation to engender higher-order function.

The BF_2 chelated-tetraarylazadipyrromethene **1** and related structural analogues have recently been reported as a class of chromophore with high absorption extinction coefficients ($70–80 \times 10^3$ M^{-1} cm^{-1}) and fluorescence quantum yields (0.23–0.36) between 650 and 750 nm (Fig. 1).[9] We have also shown that with selective positioning of prototype amine receptors this class can be utilized as a visible red and/or NIR chemosensor operating by either a photoinduced electron transfer (PET) or a charge transfer (CT) mechanism.[10] Subsequently this fluorophore class has been successfully adapted as chemosensors for analytes such as saxitoxin and mercury(II).[11]

Herein, we report the synthesis and chemosensor characteristics of a double amine receptor substitution pattern (Fig. 1 Ar^1 and Ar^2 = *p*-$(CH_3)_2NC_6H_4$). Based upon the results of an earlier model system, it was envisaged that substituting the parent chromophore molecule with two intrinsically connected amine donors would produce a more advanced molecular assembly which could generate pronounced photophysical changes as a result of a substrate recognition event by the amine substituents.[12] It was anticipated that this electron donor–acceptor double amine receptor–chromophore design would undergo pronounced spectral changes due to variance in the internal charge transfer (ICT) properties of the system in response to acid analyte. A study of the analyte responsive photophysics of this system would provide the framework for more elaborate receptors to detect other analytes.[13]

Results and discussion

Synthesis

The synthesis of our target compound **1a** was achieved in a routine four step route from acetophenone and 4-dimethylaminobenzaldehyde.[14] Condensation of the aldehyde with acetophenone gave the α,β-unsaturated ketone **2** which following conjugate addition of nitromethane provided the 1,3-diaryl-4-nitrobutan-1-one **3** in 87% yield after recrystallization (Scheme 1).

Generation of the tetraarylazadipyrromethene **4** was achieved by heating **3** with ammonium acetate in ethanol for 48 h during which time the product precipitated from solution. Filtration of the precipitate from the crude reaction mixture gave the pure product as a dark blue solid in 45% yield. A higher yield could be obtained if butanol was used as solvent (50%) but silica gel chromatography was required for purification. Compound **4** was converted to our targeted structure

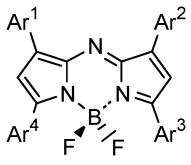

1

Fig. 1 BF_2-chelated tetraarylazadipyrromethenes.

[a] *Centre for Synthesis and Chemical Biology, School of Chemistry and Chemical Biology, University College Dublin, Belfield, Dublin 4, Ireland. E-mail: donal.f.oshea@ucd.ie; Tel: +353-(0)1-7162425*
[b] *School of Chemical Sciences, Dublin City University, Dublin 9, Ireland*

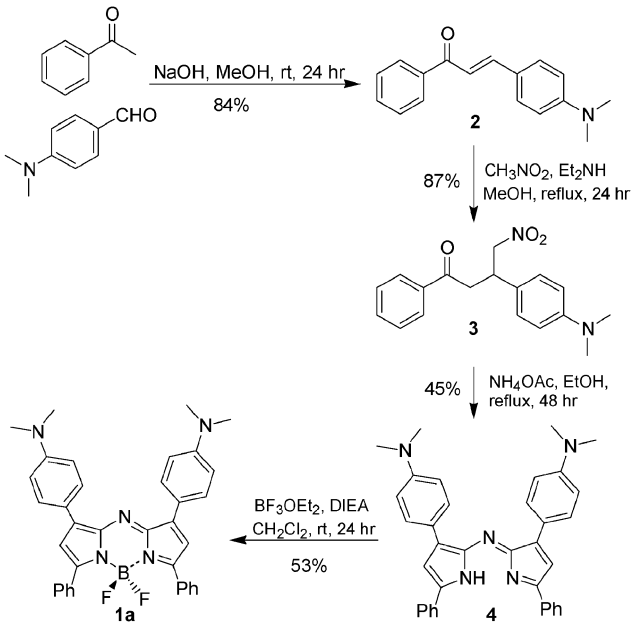

Scheme 1

1a by reaction with boron trifluoride diethyletherate and diisopropylethylamine in dichloromethane for 24 h. An isolated purified yield of 53% was obtained following chromatography on silica gel.

X-Ray crystallographic study

The crystal and molecular structure of **1a** have been determined by single-crystal X-ray diffraction both at 294 and 120 K: only the latter results will be discussed. Compound **1a** crystallizes in the triclinic system, space group ($P\bar{1}$, no. 2) with two molecules (A and B) in the asymmetric unit and though broadly similar in conformation there are quite distinct differences in the bond and torsion angles (Fig. 2 and 3). The

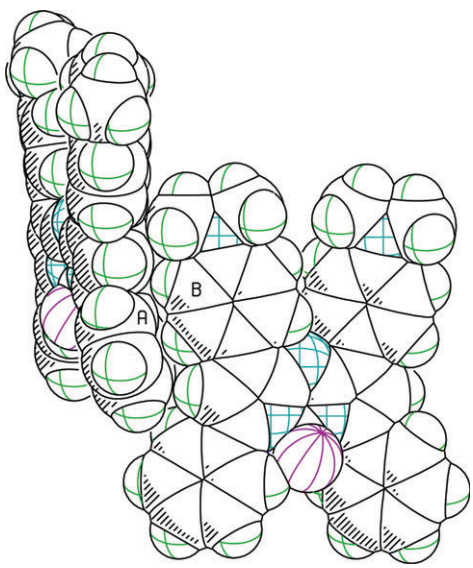

Fig. 2 A view of molecules A and B of **1a** with atoms drawn as their van der Waals spheres highlighting the C–H···π(arene) interactions between A and B.

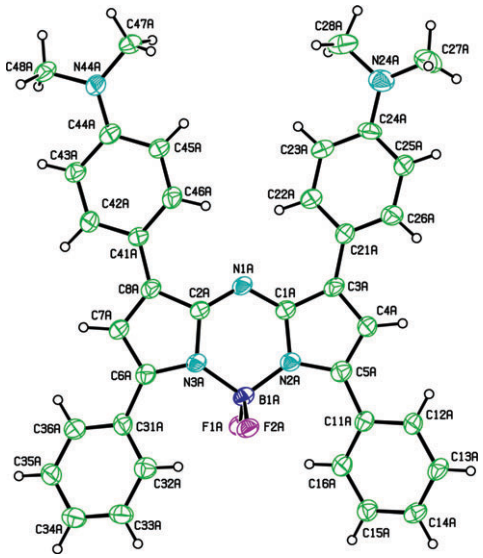

Fig. 3 Compound **1a** (molecule A) with displacement ellipsoids depicted at the 30% probability level. Weak intramolecular interactions are present involving N1A, F1A/F2A and neighbouring aromatic C–H groups (as noted in the text).

only significant intermolecular interactions involve the relatively weak C–H···N/F and C–H···π(arene) interactions of which two are noteworthy namely C42B–H42B···Cg1 [H42B···Cg1 is 2.79 Å, angle of 151°, C42B···Cg1 is 3.649(6) Å, Cg1 = centroid C11A–C16A] and C47B–H47E···$Cg2^i$ [H47E···$Cg2^i$ is 2.82 Å, angle of 137°, C47B···$Cg2^i$ is 3.604(6) Å, Cg2 = centroid C31B–C36B, symmetry operation $i = 1 - x, -y, 1 - z$] (Fig. 2). These weak interactions and packing forces combine to enforce subtle differences between molecules A and B in the solid state.

The interactions in **1a** mainly comprise intramolecular aromatic C–H···F involving the BF_2 moiety. The interactions for molecule A are H16A···F1A at 2.16 Å (C16A···F1A is 3.046(6) Å, angle of 152°) and H32A···F2A at 2.15 Å (C32A···F2A is 3.006(7) Å, angle of 150°): molecule B is similar with H16B···F1B 2.17 Å (C16B···F1B is 3.020(5) Å, angle of 150°) and H32B···F2B 2.20 Å (C32B···F2B is 3.047(6) Å, angle of 148°) (Fig. 3).

The NMe_2 groups are representative with a separation of *ca.* 0.6 Å for the N···N non-bonded distances of 7.617(7) and 7.041(6) Å in molecules A and B, respectively. There are no discernible differences in the internal bond lengths between molecules A and B primarily due to the data quality: the esds are large and preclude meaningful one-for-one comparisons. However, there are distinct differences in atom separation distances in the molecules as a result of subtle conformational differences. In molecule A, the C3A···N24A and C8A···N44A distances are 5.682(8) and 5.649(7) Å [5.666(8), 5.646(7) Å in B], but this is not significant for elongation or shortening along the C–C_6H_4–NMe_2 groups in either molecule. A more distinct difference is the B···N distances for B1A···N24A/N44A being 9.215(9)/9.209(8) Å (similar to B1B···N44B, 9.190(8) Å) but longer by 0.08 Å in comparison to B1B···N24B at 9.128(9) Å. Therefore, molecules A and B differ subtly and examination of the N···N distances between

the *para*-disubstituted C–C_6H_4–NMe_2 rings highlights these subtleties with N24A···N44A 7.617(7) Å and N24B···N44B 7.041(6) Å, indicating an opening up or bending of these groups relative to one another (the N24···N1···N44 angles in A, B are 70.04(7), 65.39(7)°). The distortion can also be observed in the torsion angles where the N24···C3···; C8···N44 angles for A, B differ by 10° (−0.83(13)° in A and 9.20(14)° in B).

The three central fused-rings of **1a** (comprising 12 atoms, 4 of which are common to the five/six-membered fused-ring, discounting the F atoms) are essentially co-planar (though with a slight 'ruffling') with the maximum deviation for any non-hydrogen atom in either of the two five-membered C_4N or the six-membered BC_2N_3 rings in molecules A, B is for C1A, C3A by 0.020(3) Å in C_4N and 0.026(3) Å for C1B in the BC_2N_3 core in B (Fig. 4).

The range of interplanar angles between the five- and six-membered [C_4N/BC_2N_3] rings is from 4.6(3) to 6.4(3)°, highlighting the essentially co-planar nature of the 12 atoms in the central fused-ring moieties.[9] The C_6H_5 (phenyl) ring orientations differ with angles of 17.4(3)° (A) and 13.9(2)° (B) for the [C11–C16]/[C31–C36] planes, while the NMe_2 substituted C_6 ring planes are oriented at 10.5(3)° (A) and 9.4(2)° (B).

The four NMe_2 (molecules A and B) groups differ considerably, both in their twist angles with respect to the C_6 rings, but also due to pyramidalisation effects at the N atoms. A convenient measure of pyramidalisation is the distance from the N atom to the C_3, [C_{Me}/C_{arom}/C_{Me}], plane (this is 0.0 Å when the N and 3C atoms are co-planar). In **1a**, the range is from 0.003(5) Å (for N44B···C_3) to 0.137(6) Å (for N24A···C_3), indicating a range of geometries within the NMe_2 groups. A Cambridge Structural Database (CSD) analysis for C–C_6–NMe_2 moieties in a range of 300+ molecules shows a direct correlation between increasing C–N_{Me} bond length (increasing single bond character), increasing C_6/NMe_2 twist angle (from 0°) and pyramidalisation at the N atom (increasing N···C_3 plane distance).[12] In **1a**, the longest C–N_{Me} distance is 1.384(7) Å for C24A–N24A [range of 1.353(7)–1.373(6) Å for the three remaining C–N distances involving N44A, N24B, N44B]: a corresponding twist of 14.0(7)° at N24A [2.1(5)–4.3(4)° at N44A, N24B, N44B], and a N24A···C_3 distance of 0.137(6) Å [0.003(5)–0.065(6) Å for N44A, N24B, N44B···C_3]. In **1a** our results follow the observed trend observed in the CSD analysis for C–C_6–NMe_2 systems described above. Increasing single bond character in the C–N bond (C–N lengthening) correlates well with increased twisting away from C_6/NMe_2 co-planarity and with larger pyramidalisation at the N atom (greater N···C_3 plane distance). Therefore, the resulting and decreasing ability of the lone pair of electrons on the N atom to participate in conjugation with the aromatic C_6 group is observed through (a) longer C–N bond lengths, (b) increased twisting from co-planarity and (c) increased N atom pyramidalisation. These effects at the C–NMe_2 chromophore can have a profound effect on the photophysical properties of a system in the solid state and in the solution if there is a measure of steric influence restricting rotation of the NMe_2 and other pendant groups.

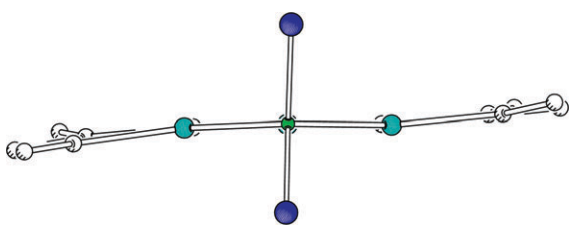

Fig. 4 A view along the B···N axis of the central core non-hydrogen atoms in **1a** (molecule A) with the hydrogen atoms and peripheral C/N atoms removed for clarity.

Spectroscopic study

Aqueous solutions of **1a**, suitable for pH titrations, were made using the emulsifier Cremophor EL (CrEL), a commonly used non-ionic surfactant exploited as a formulating agent for poorly water-soluble pharmaceuticals.[15] Examination of the excited state response of aqueous formulated solutions of **1a** to varying acidic conditions were carried out. We were pleased to observe virtually complete quenching of the fluorescence in the pH range where the amine receptor remained unprotonated (Fig. 5, red trace). Upon protonation, the fluorescence spectrum showed a strong proton induced fluorescence enhancement with a wavelength of maximum fluorescence at 685 nm (Fig. 5, green trace). A sigmoidal plot of pH *vs.* fluorescence intensity predicted an apparent pK_a of less than 1.0 (Fig. 5, inset). This value is indicative of a strong coupling of the receptor and fluorophore sub-units, though it should be noted that pK_a values in a micellar microenvironment are often lower than might be anticipated. Significantly, the enhancement of fluorescence intensity was greater than 250-fold between the chemosensor off and on positions. The co-planarity of the receptors and the fluorophore of chemosensor **1a** facilitates a donor–acceptor CT interaction between the anilino lone pairs of electrons and the fluorophore in the unprotonated state, which gives rise to highly efficient quenching of the fluorescence emission. This is further endorsed by analysis of the absorption spectrum of **1a**. Unprotonated **1a** displays strong CT characteristics with three bands between 500 and

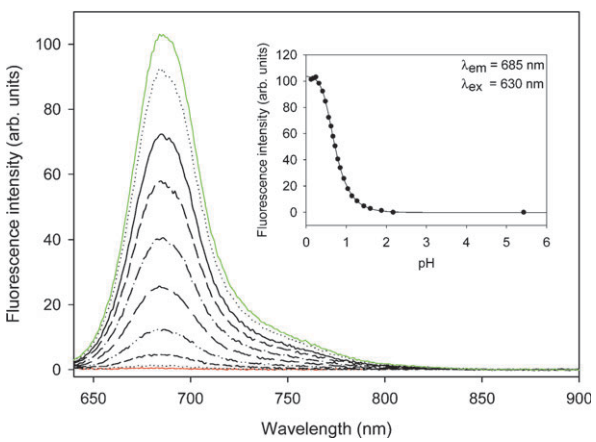

Fig. 5 pH responsive fluorescence spectra of **1a** (excitation 630 nm, 1×10^{-6} M) in H_2O/CrEL, I_{NaCl} = 150 mmol L^{-1}. The pH values in order of decreasing intensity are 0.25, 0.40, 0.55, 0.65, 0.80, 0.95, 1.15, 1.45, 1.90 and 5.45. Inset shows sigmoidal plot predicting an apparent pK_a value of <1.

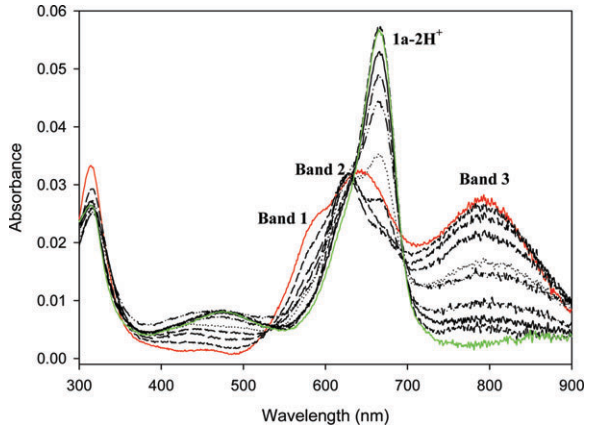

Fig. 6 pH responsive absorbance spectra of **1a** (1×10^{-6} M) in H_2O/CrEL, I_{NaCl} = 150 mmol L^{-1}. The pH values in order of decreasing intensity of band 3 are 5.45, 1.90, 1.45, 1.15, 0.95, 0.80, 0.65, 0.55, 0.40 and 0.25.

900 nm (Fig. 6, red trace). Computational deconvolution of bands 1 and 2 gave maxima at 586 and 620 nm, respectively (Fig. 7, inset). At pH values greater than 2, no spectral shifts are demonstrated by **1a**. At pH values <2, bands 1 and 3 can be clearly seen to progressively reduce in intensity and a new band centred at 665 nm for **1a-2H**$^+$ appears (Fig. 6, green trace).

A plot of pH *vs.* intensity of absorbance bands 1 and 3 clearly demonstrates the double protonation event occurring as a consequence of the two amine receptors. Two sigmoidal response curves were calculated for band 1 and 3 (red and blue, respectively) predicting an apparent pK_a of 1.4 for the first protonation and <1 for the second (Fig. 7) As the pK_a of the second protonation was similar to that observed in the fluorescence titration this would indicate that it is only upon the second protonation that the fluorescence of **1a** is re-established. This is clearly demonstrated in a ratiometric plot of disappearance of the absorption band at 789 nm *vs.* emergence of fluorescence intensity giving an intersect at the pK_a value (Fig. 8).[16]

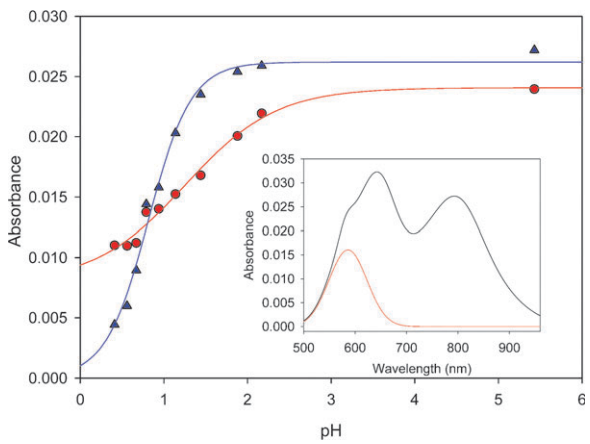

Fig. 7 pH profiles for disappearance of band 1 at 586 nm (red circles, experimental; line, sigmoidal fit) and band 3 at 789 nm (blue triangles, experimental; line, sigmoidal fit) of **1a** (1×10^{-6} M). Inset shows resolved component peaks of the absorbance spectrum generated with PeakFit software.

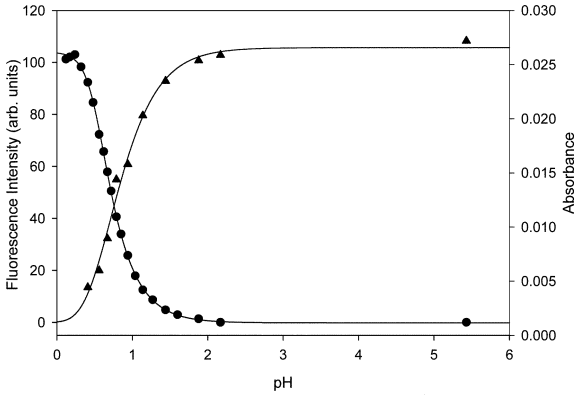

Fig. 8 Ratiometric pH profile of **1a** (1×10^{-6} M) for increase of fluorescence emission at 685 nm (● experimental; — sigmoidal fit) and decrease of absorbance band 3 at 789 nm (▲ experimental; — sigmoidal fit) for **1a**.

The solvent effects on the steady state fluorescence properties of **1a** and **1a-2H**$^+$ are shown in Fig. 9. It is remarkable to note that in all the organic solvents studied, polar and non-polar, the fluorescence of **1a** is almost completely quenched at the respective emission wavelengths of **1a-2H**$^+$. This is in contrast to other aniline substituted fluorosensors including the aniline substituted 4,4-difluoro-4-bora-3a,4a-diaza-*s*-indacenes (BODIPY class) which exhibit pronounced solvent dependent fluorescence quantum yields with high yields recorded in non-polar solvents.[17] In the less polar solvents cyclohexane, chloroform and toluene the unprotonated fluorosensor shows a low intensity long wavelength emission ranging from 795 to 822 nm, attributed to emission from a CT species. The fluorescence spectra of **1a-2H**$^+$ (TFA added to solution of **1a**) show some solvent polarity dependency with positions of maximum fluorescence varying from 677 nm in ethanol to 692 nm in toluene (Table 1). Full widths at half maximum (FWHM) in all solvents are narrow ranging from 39 to 43 nm. All solvents show excellent fluorescent enhancement factors (FEF) with the unprotonated fluorosensor in the more polar solvents showing complete quenching of fluorescence.

The absorption spectrum of **1a** in organic solvents exhibited three distinct bands, as was observed for the aqueous

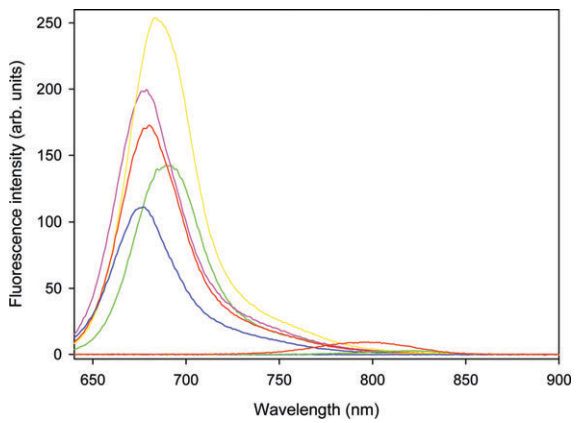

Fig. 9 Fluorescence spectra of **1a** and **1a-2H**$^+$ (TFA added) (excitation 630 nm; 5×10^{-7} M) in acetonitrile (pink), chloroform (yellow), cyclohexane (red), ethanol (blue) and toluene (green).

Table 1 Spectroscopic fluorescence data for **1a-2H**$^+$

Solvent[a]	λ_{max}/nm	FWHM/nm	FEF
Cyclohexane	680	39	180
Toluene	692	43	240
Chloroform	684	41	>250
Ethanol	677	40	>250
Acetonitrile	679	40	>250

[a] Room temperature.

Table 2 Spectroscopic absorbance data for **1a**

Solvent[a]	Band 1/nm	Band 2/nm	Band 3/nm
Cyclohexane	576	613	744
Toluene	574	625	763
Chloroform	572	625	770
Ethanol	569	631	772
Acetonitrile	572	648	799

[a] Room temperature.

formulated solutions. The shortest wavelength band was more distinct in polar solvents such as acetonitrile than cyclohexane (Fig. 10). The absorbance bands 2 and 3 show a strong positive solvatochromism in proportion to increasing solvent polarity, bathochromically shifting to 648 and 799 nm in acetonitrile when compared to 613 and 744 nm in cyclohexane (Table 2). Specifically band 3 exhibited the strongest positive solvatochromism with increasing solvent polarity, which is a common characteristic of CT compounds.

Conclusions

In conclusion, we have outlined a facile synthesis to a new class of ratiometric fluorometric and colourimetric chemosensor with potential to be exploited and adapted to suit a diverse range of analytical, imaging and material applications. Specifically the low pH range in which sensor response occurs indicates that this platform would be suitable for detection of other analytes at physiological pH. Chemosensor performance is excellent with large off/on fluorescence intensity responses and low microenvironment polarity effects. In addition the described synthetic route would readily allow for analogues functionalised with other substrate specific receptors to be generated.

Experimental

General

^{1}H NMR spectra were recorded on a Varian FT spectrometer at 300 MHz and ^{13}C NMR spectra at 75 MHz, in $CDCl_3$ with tetramethylsilane as the internal standard. All chemical shifts are quoted in δ (ppm) and coupling constants in Hz. Melting points were determined on a Reichert Thermovar melting point platform. Mass spectral analyses were performed on a Micromass Quattro Micro. IR spectra were recorded on a Mattson Instruments Galaxy series FT-IR 3000 spectometer. Absorption spectra were recorded on a Varian Cary 50 UV-visible spectrophotometer. Fluorescence spectra were recorded on a Cary Eclipse spectrofluorometer. Elemental analyses were carried out at the microanalytical laboratory, University College Dublin.

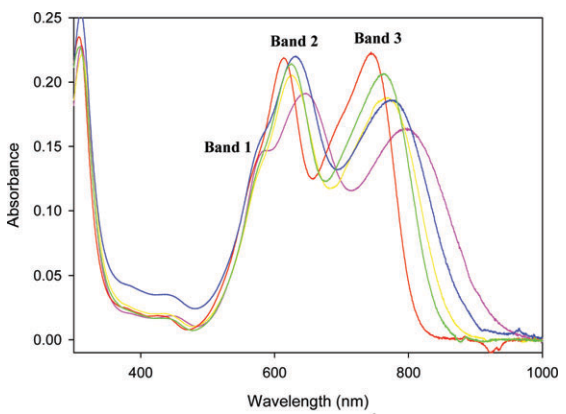

Fig. 10 Absorbance spectra of **1a** (5×10^{-6} M) in acetonitrile (pink), chloroform (yellow), cyclohexane (red), ethanol (blue) and toluene (green).

3-(4-Dimethylaminophenyl)-1-phenylpropenone (2). 4-Dimethylaminobenzaldehyde (10.0 g, 67 mmol), 1-phenylethanone (8.05 g, 67 mmol) and three NaOH pellets were dissolved in methanol (100 mL) and stirred at room temperature until a heavy precipitate formed (24 h). The precipitate was isolated by filtration and washed with cold methanol to give the product without any further purification, as a bright yellow solid of **2** (14.07 g, 84%), mp 110–112 °C. ^{1}H NMR (300 MHz, $CDCl_3$) δ 7.98–8.02 (m, 2H), 7.79 (d, J = 15.5 Hz, 1H), 7.43–7.56 (m, 5H), 7.32 (d, J = 15.5 Hz, 1H), 6.64–6.69 (m, 2H), 3.00 (s, 6H). ^{13}C NMR (75 MHz, $CDCl_3$) δ 190.8, 152.3, 146.0, 139.3, 132.3, 130.6, 128.7, 128.5, 122.9, 117.1, 112.0, 40.33. IR (KBr disc): 1649 cm^{-1}. ES-MS: m/z $[M + H]^+$ 252.1. Anal. Calc. for $C_{17}H_{17}NO$: C, 81.24; H, 6.82; N, 5.57. Found: C, 80.95; H, 6.82; N, 5.49%.

3-(4-Dimethylaminophenyl)-4-nitro-1-phenylbutan-1-one (3). 3-(4-Dimethylaminophenyl)-1-phenylpropenone **2** (7.0 g, 28.0 mmol) was dissolved in anhydrous methanol (75 mL), nitromethane (8.5 g, 140 mmol) and diethylamine (10.22 g, 140 mmol) were added, and the reaction was heated under reflux for 24 h. The reaction mixture was allowed to cool to room temperature, acidified with 1 M hydrochloric acid and the resulting precipitate was isolated by filtration. Recrystallization from methanol gave the product **3** as a yellow solid (7.6 g, 87%), mp 113–115 °C. ^{1}H NMR (300 MHz, $CDCl_3$) δ 7.88–7.92 (m, 2H), 7.51–7.57 (m, 1H), 7.40–7.46 (m, 2H), 7.09–7.14 (m, 2H), 6.63–6.68 (m, 2H), 4.76 (dd, J = 12.3, 6.8 Hz, 1H), 4.61 (dd, J = 12.3, 7.9 Hz, 1H), 4.11 (m, 1H), 3.44 (dd, J = 6.1, 17.0 Hz), 3.36 (dd, J = 7.6, 17.0 Hz), 2.89 (s, 6H). ^{13}C NMR (75 MHz, $CDCl_3$) δ 197.5, 150.3, 136.8, 133.6, 128.9, 128.3, 128.3, 126.6, 113.0, 80.2, 42.0, 40.6, 38.8. IR (KBr disc): 1680, 1546 cm^{-1}. ES-MS: m/z $[M + H]^+$ 313.2. Anal. Calc. for $C_{18}H_{20}N_2$: C, 69.21; H, 6.45; N, 8.97. Found: C, 69.40; H, 6.39; N, 8.83%.

[3-(4-Dimethylaminophenyl)-5-phenyl-1*H*-pyrrol-2-yl][3-(4-dimethylaminophenyl)-5-phenylpyrrol-2-ylidene]amine (4). A 100 mL round-bottomed flask was charged with 3-(4-di-

methylaminophenyl)-4-nitro-1-phenylbutan-1-one **3** (1.0 g, 3.21 mmol), ammonium acetate (8.7 g, 112 mmol) and ethanol (20 mL) and heated under reflux for 48 hours. During the course of the reaction, the product precipitated from the reaction mixture. The reaction was cooled to room temperature, filtered and the isolated solid washed with cold ethanol (2 × 10 mL) to yield the product **4** as a blue–black solid (0.40 g, 46%), mp 248–250 °C. ^{1}H NMR ($CDCl_3$) δ 8.04 (d, J = 9.0 Hz, 4H), 7.94 (d, J = 7.0 Hz, 4H), 7.40–7.53 (m, 6H), 7.05 (s, 2H), 6.78 (d, J = 9.0 Hz, 4H), 3.04 (s, 6H), (NH not observed). ^{13}C NMR ($CDCl_3$) δ 154.8, 150.4, 149.8, 143.1, 132.9, 130.5, 129.7, 129.2, 126.6, 122.9, 112.2, 111.9, 40.6. IR (KBr disc): 3462, 1607 cm^{-1}. λ_{max} ($CHCl_3$): 623 nm. HRMS: calc. for $C_{36}H_{34}N_5$ $[M + H]^+$: 536.2814, found: 536.2806. Anal. Calc. for $C_{36}H_{33}N_5$: C, 80.72; H, 6.21; N, 13.07. Found: C, 80.44; H, 6.14; N, 13.10%.

BF_2-chelated-[3-(4-dimethylaminophenyl)-5-phenyl-1*H*-pyrrol-2-yl][3-(4-dimethylaminophenyl)-5-phenylpyrrol-2-ylidene]amine (1a). [3-(4-Dimethylaminophenyl)-5-phenyl-1*H*-pyrrol-2-yl]-[3-(4-dimethylaminophenyl)-5-phenylpyrrol-2-ylidene]amine **4** (0.1 g, 0.186 mmol) was dissolved in dry CH_2Cl_2 (50 mL), treated with diisopropylethylamine (0.14 mL, 0.78 mmol) and boron trifluoride diethyl etherate (0.14 mL, 1.4 mmol), and stirred at room temperature under nitrogen for 24 h. The mixture was washed with water (2 × 50 mL), and organic layer was dried over sodium sulfate and evaporated to dryness. Purification by column chromatography on silica gel eluting with CH_2Cl_2–hexane (3 : 1) gave the product **1a** as a metallic brown solid (0.057 g, 53%), mp 258–261 °C. ^{1}H NMR ($CDCl_3$) δ 8.07 (dd, J = 2.0, 7.0 Hz, 4H), 7.98–8.01 (m, 4H), 7.41–7.46 (m, 6H), 6.81 (s, 2H), 6.76 (dd, J = 2.0, 7.0 Hz, 4H), 3.07 (s, 12H). ^{13}C NMR ($CDCl_3$) δ 158.1, 151.3, 145.8, 144.0, 132.7, 131.1, 130.2, 129.5, 128.5, 121.5, 115.4, 112.2, 40.4. IR (KBr disc): 1603, 1487 cm^{-1}. EI-MS: m/z 583. HRMS: calc. for $C_{36}H_{33}BF_2N_5$ $[M + H]^+$: 584.2797, found: 584.2813. Anal. Calc. for $C_{36}H_{32}BF_2N_5$: C, 74.10; H, 5.53; N, 12.00. Found: C, 72.52; H, 5.55; N, 11.56%. Crystals were grown by the slow evaporation of a chloroform solution.

X-Ray data collection, structure solution and refinement

Data were collected on a Siemens-Bruker P4 diffractometer for **1a** at room temperature (294 K) and processed using the XSCANS suite of programs.[18] A low-temperature study was also subsequently undertaken of **1a** at 120 K using an Enraf-Nonius diffractometer at the University of Southampton (ESPRC service) and data were processed using the SMART suite of programs.[19] Compound **1a** crystallizes in the triclinic system ($P\bar{1}$, no. 2) with two molecules (A/B) in the asymmetric unit. Solution and refinement was undertaken using SHELXS97 and SHELXL97[20] and the graphics generated with PLATON.[21]

No disorder is present in **1a** but an initial study of a very weakly diffracting crystal at room temperature (294 K) provided only gross conformation details and resulted in a high R-factor: however, the geometry looks reasonable, though with geometric data having rather high esds (s.u.'s). Better quality crystals of **1a** were subsequently obtained *via* several recrystallization experiments and data were subsequently collected on an Enraf-Nonius CCD diffractometer at 120 K for comparison purposes. A lower R-factor with improved lower esds were obtained for a detailed comparison of the two independent molecules (A and B) in the asymmetric unit. Brief details of the 294 K dataset of **1a** are listed and all further discussion refers to the low-temperature 120 K dataset of **1a**. All non-hydrogen atoms were refined using anisotropic displacement parameters and hydrogen atoms were treated as riding atoms using the SHELXL97 defaults at the appropriate temperatures (294 and 120 K).

Crystal data for 1a at 294 K. $C_{36}BF_2N_5$, M = 583.48, triclinic, space group $P\bar{1}$, a = 10.372(10), b = 14.250(13), c = 21.168(15) Å, α = 106.19(8), β = 91.03(11), γ = 92.06(9)°, V = 3001(5), Z = 4, μ = 0.086 mm^{-1}; 1492 reflections with $I > 2\sigma(I)$, $R(I > 2\sigma(I))$ = 0.1541, $wR(I > 2\sigma(I))$ = 0.3428.

Crystal data for 1a at 120 K. $C_{36}BF_2N_5$, M = 583.48, triclinic, space group $P\bar{1}$, a = 10.2169(7), b = 14.0769(8), c = 21.0039(15) Å, α = 105.548(2), β = 91.046(2), γ = 92.138(5)°, V = 2907.0(3), Z = 4, μ = 0.088 mm^{-1}; 3569 reflections with $I > 2\sigma(I)$, $R(I > 2\sigma(I))$ = 0.0862, $wR(I > 2\sigma(I))$ = 0.1415.

CCDC reference numbers 646558 (294 K) and 646559 (120 K). For crystallographic data in CIF or other electronic format see DOI: 10.1039/b713020a

Formulation

Compound **1a** (0.005 mmol) was dissolved in THF (1 mL) and Cremophor EL (0.1 mL) added. The mixture was sonicated for 30 min followed by removal of the THF under reduced pressure. The resulting blue oil was dissolved in 25 mL of saline solution (2.19 g NaCl in 250 mL water) and filtered through an Acrodisc 25 mm syringe filter (with 0.2 μm HT Tuffryn membrane). Final concentration was checked by UV-visible spectral analysis.

UV-visible and fluorescence procedures

Solvents used were spectrophotometric grade chloroform, which was distilled over potassium carbonate prior to use, spectrophotometric grade acetonitrile and HPLC grade cyclohexane. UV-visible spectra were determined from a 1 cm path quartz cell at room temperature. Baseline corrected UV-visible spectra were collected between 250 and 1100 nm. Fluorescence spectra were determined at room temperature from a 1 cm path quartz cell with excitation and emission slit widths of 5 nm. FEF = fluorescence enhancement factor (I_{Fmax}/I_{Fmin}).

Acknowledgements

This work was funded under the Program for Research in Third-Level Institutions administered by the HEA. S. O. McD. thanks the Irish Research Council for Science, Engineering and Technology for a studentship. J. F. G. thanks Dublin City University for the purchase of a Siemens P4 diffractometer and computer system. Thanks to Dr D. Rai of the CSCB Mass Spectrometry Centre for mass analyses and

ESPRC service (University of Southampton) for collecting a low temperature dataset.

References

1 H. Mustroph, M. Stollenwerk and V. Bressau, *Angew. Chem., Int. Ed.*, 2006, **45**, 2016.
2 K. Y. Law, *Chem. Rev.*, 1993, **93**, 449.
3 K. Rurack, M. Kollmannsberger and J. Daub, *Angew. Chem., Int. Ed.*, 2001, **40**, 385.
4 For examples, see: (*a*) J.-M. Zen and G. Patonay, *Anal. Chem.*, 1991, **63**, 2934; (*b*) Z. Zhang and S. Achilefu, *Chem. Commun.*, 2005, 5887.
5 A. Gómez-Hens and M. P. Aguilar-Caballos, *Trends Anal. Chem.*, 2004, **23**, 127.
6 V. Ntziachristos, J. Ripoll, L. V. Wang and R. Weissleder, *Nat. Biotechnol.*, 2005, **23**, 313.
7 R. Weissleder, *Nat. Biotechnol.*, 2001, **19**, 316.
8 A. Mishra, R. K. Behera, P. K. Behera, B. K. Mishra and G. B. Behera, *Chem. Rev.*, 2000, **100**, 1973.
9 (*a*) J. Killoran, L. Allen, J. F. Gallagher, W. M. Gallagher and D. F. O'Shea, *Chem. Commun.*, 2002, 1862; (*b*) A. Gorman, J. Killoran, C. O'Shea, T. Kenna, W. M. Gallagher and D. F. O'Shea, *J. Am. Chem. Soc.*, 2004, **126**, 10619; (*c*) S. O. McDonnell, M. J. Hall, L. T. Allen, A. Byrne, W. M. Gallagher and D. F. O'Shea, *J. Am. Chem. Soc.*, 2005, **127**, 16360; (*d*) W. M. Gallagher, L. T. Allen, C. O'Shea, T. Kenna, M. Hall, J. Killoran and D. F. O'Shea, *Br. J. Cancer*, 2005, **92**, 1702; (*e*) D. F. O'Shea, J. Killoran and W. M. Gallagher, *US Pat.*, 7220732, 2007.
10 For PET examples, see: (*a*) J. Killoran and D. F. O'Shea, *Chem. Commun.*, 2006, 1503; (*b*) M. J. Hall, L. T. Allen and D. F. O'Shea, *Org. Biomol. Chem.*, 2006, **4**, 776. For CT examples, see: ; (*c*) S. O. McDonnell and D. F. O'Shea, *Org. Lett.*, 2006, **8**, 3493.
11 (*a*) R. E. Gawley, H. Mao, M. Mahbubul Haque, J. B. Thorne and J. S. Pharr, *J. Org. Chem.*, 2007, **72**, 2187; (*b*) A. Coskun, M. Deniz Yilmaz and E. U. Akkaya, *Org. Lett.*, 2007, **9**, 607.
12 J. Killoran, J. F. Gallagher, P. V. Murphy and D. F. O'Shea, *New J. Chem.*, 2005, **29**, 1258.
13 (*a*) A. P. de Silva, H. Q. N. Gunaratne, T. Gunnlaugsson, A. J. M. Huxley, C. P. McCoy, J. T. Rademacher and T. E. Rice, *Chem. Rev.*, 1997, **97**, 1515; (*b*) J. H. Hartley, T. James and C. J. Ward, *J. Chem. Soc., Perkin Trans. 1*, 2000, 3155.
14 For related synthesis, see; M. J. Hall, S. O. McDonnell, J. Killoran and D. F. O'Shea, *J. Org. Chem.*, 2005, **70**, 5571.
15 H. Gelderblom, J. Verweij, K. Nooter and A. Sparreboom, *Eur. J. Cancer*, 2001, **37**, 1590.
16 For examples of ratiometric sensors, see: (*a*) J. V. Mello and N. S. Finney, *Angew. Chem., Int. Ed.*, 2001, **40**, 1536; (*b*) K. Choi and A. D. Hamilton, *Angew. Chem., Int. Ed.*, 2001, **40**, 3912; (*c*) Z. Xu, X. Qian and J. Cui, *Org. Lett.*, 2005, **7**, 3029.
17 For examples, see: (*a*) K. Rurack, M. Kollmannsberger and J. Daub, *New J. Chem.*, 2001, **25**, 289; (*b*) K. Rurack, M. Kollmannsberger and J. Daub, *Angew. Chem., Int. Ed.*, 2001, **40**, 385.
18 Siemens Bruker AXS 1994, XSCANS Software, Ver. 2.2 Madison, WI, USA.
19 Bruker SMART, SAINT and SADABS, Bruker AXS Inc., Madison, WI, USA, 2000.
20 (*a*) G. M. Sheldrick, *SHELXS97 and SHELXL97*, University of Göttingen, Germany; (*b*) P. McArdle, *J. Appl. Crystallogr.*, 1995, **28**, 65.
21 A. L. Spek, *J. Appl. Crystallogr.*, 2003, **36**, 7.